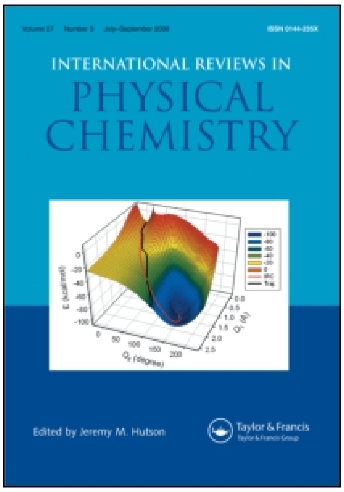

International Reviews in Physical Chemistry
Publication details, including instructions for authors and subscription information:
http://www.informaworld.com/smpp/title~content=t713724383

Sticking of molecular hydrogen on simple, noble and transition metal surfaces

A. Winkler[a]; K. D. Rendulic[a]
[a] Institut für Festkörperphysik, Technische Universität Graz, Graz, Austria

To cite this Article Winkler, A. and Rendulic, K. D.(1992) 'Sticking of molecular hydrogen on simple, noble and transition metal surfaces', International Reviews in Physical Chemistry, 11: 1, 101 — 133
To link to this Article: DOI: 10.1080/01442359209353267
URL: http://dx.doi.org/10.1080/01442359209353267

INTERNATIONAL REVIEWS IN PHYSICAL CHEMISTRY, 1992, VOL. 11, NO. 1, 101–133

Sticking of molecular hydrogen on simple, noble and transition metal surfaces

by A. WINKLER and K. D. RENDULIC
Institut für Festkörperphysik, Technische Universität Graz,
Petersgasse 16, A-8010 Graz, Austria

The dynamics of adsorption for molecular hydrogen on different metal surfaces (Ni, Cu, Al) is discussed in this review. Surface parameters like geometric and electronic structure, surface defects and impurities, surface coverage and surface temperature as well as gas parameters like translational, vibrational and rotational energy and angle of incidence influence the sticking probability of H_2. On transition metal surfaces the sticking coefficient is rather high, whereas on noble and simple metals the sticking coefficient is exceedingly small. Only translationally and/or vibrationally hot molecules are able to adsorb on the latter surfaces. These features are discussed in the context of appropriate potential energy surfaces which govern the adsorption process. Experimental methods to determine absolute sticking coefficients as function of different gas parameters are also described.

1. Introduction

Gas–surface interactions have attracted enormous interest in the last decades. The main reason is that many technologically important processes are based on or influenced by gas–surface reactions. Examples are heterogeneous catalysis, microelectronics or fusion technology. The second important reason is that only recently the necessary instrumentation has been made available to study gas–surface processes in more detail. In particular ultrahigh vacuum technology and highly sophisticated analytical methods have contributed to the enormous progress in surface physics.

Whereas for probing the static properties of adsorbates (structure, energetics, etc.) a considerable number of techniques are available, the investigation of the dynamics of adsorption is still in its infancy. Although a vast amount of experimental data can be found in the literature concerning the adsorption kinetics, in many cases the experiments have not been performed under well defined conditions. This is not only true for the characterization of the surface itself (e.g. structures, defects, impurities) but also for the gas phase characterization (e.g. internal energy of the molecules, angle of incidence).

In this review we will comprehensively deal with the adsorption dynamics of hydrogen on metal surfaces. For these adsorption systems a relatively large number of reliable experimental data exists and also theoretical background is available to some extent (see references in Christmann (1988)). In the first section we present a general description of the sticking coefficient and its dependence on surface and gas parameters. The sticking coefficient is the quantity which essentially characterizes the adsorption dynamics. In the next section we briefly discuss the experimental methods and requirements to determine quantitatively integral and differential sticking coefficients. In the following sections we finally present experimental data on the sticking coefficient of hydrogen on transition metal (nickel), noble metal (copper) and simple metal (aluminium) surfaces. Due to the different electronic structure of these

0144–235X/92 $3·00

metals the sticking probability exhibits considerable variations on these surfaces. The experimental data will be discussed within the context of existing theoretical models, using the appropriate potential energy surfaces to characterize the adsorption process.

2. The sticking coefficient

2.1. *Potential energy surfaces and the sticking coefficient*

The sticking coefficient (probability) is defined as the ratio of the adsorption rate to the impingement rate of the gas particles on the surface. It is generally assumed that an isotropic gas with a Maxwellian distribution is supplied to the surface. Obviously, in this experiment one integrates over the polar and azimuthal angles of incidence, over the velocity distribution of the molecules and over their internal state distribution. We therefore call this quantity the *integral or conventional sticking coefficient* $\bar{S}$. For comparison with theoretical models it is desirable to measure *differential sticking coefficients*, that means sticking coefficients as a function of one or more of the parameters mentioned above. The sticking coefficient is actually a function of *surface parameters* like surface geometric structure, surface electronic structure, surface defects and impurities, surface coverage and surface temperature. In addition, the point of impact within the surface unit cell is of great importance. It also depends on a number of *gas parameters* like angle of incidence, translational, vibrational and rotational energy and also on the orientation of the rotating and vibrating molecule with respect to the surface.

For a theoretical description of the adsorption dynamics (i.e. the differential sticking coefficient) the interaction potential between the gas particle and the surface atoms has to be obtained. As a next step the probability of adsorption of the gas particles approaching the surface can be determined. It is the particular shape of the potential energy surfaces (PES) that determines the rate of adsorption. A typical two-dimensional energy level diagram obtained from cluster calculations (Harris *et al.* 1988, Hand and Holloway 1989) is given in figure 1. The two parameters defining the potential energy are the distance between the surface and the molecular axis and the intramolecular separation of the two hydrogen atoms. If the molecule is far away from the surface the potential is simply given by the vibrational potential of the molecule. The molecule approaches the surface through the entrance channel of adsorption (region I). Near the surface the H–H bonds are successively weakened and the H–metal bonds are formed (reaction zone). Finally the activation barrier (seam or col in figure 1) is transgressed and two separate hydrogen atoms leave the region of elevated potential energy through the exit channel of adsorption (region II). If one follows the potential diagram from the molecular state to the dissociated state along the energetically lowest possible trajectory (the reaction path) one gets the well known one-dimensional representation of the potential energy diagram (figure 2) already proposed by Lennard-Jones (1932).

Determination of the sticking coefficient for a molecule feeling a distinct potential energy is usually done by either classical trajectory calculations (Tully 1980, Lee and DePristo 1986) or using strict quantum mechanical treatments (Halstead and Holloway 1990, Küchenhoff *et al.* 1991). Examples for a classical trajectory calculation (figure 3) and a quantum mechanical wave packet treatment (figure 4) are shown. It is clear that it is very difficult and presently impossible to include all the parameters (e.g. molecular orientation, quantum state of the molecule) in the theoretical calculation. Up to now in the construction of the PES only a restricted set of parameters is used. The molecule is assumed to approach the surface perpendicular, with the molecule axis

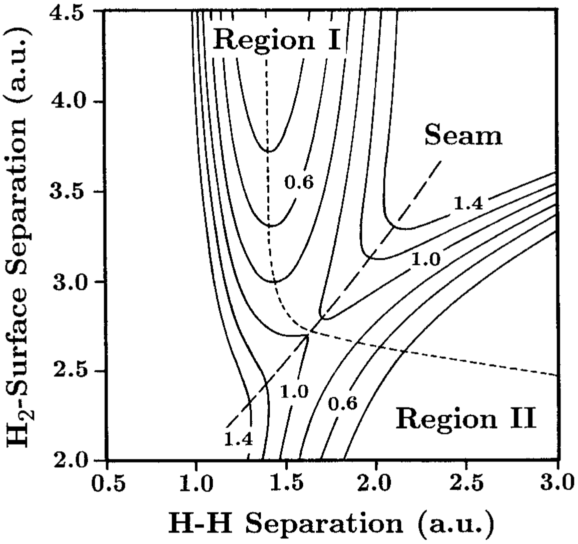

Figure 1. Two-dimensional energy level diagram for the interaction of H_2 with a metal surface from Hand and Holloway 1989. Region I represents the potential energy of the free H_2 molecule, region II the potential energy of the adsorbed hydrogen atoms. Both regions are separated by the seam. The dashed line denotes the minimum energy reaction path, the numbers in the diagram represent the potential energies in eV.

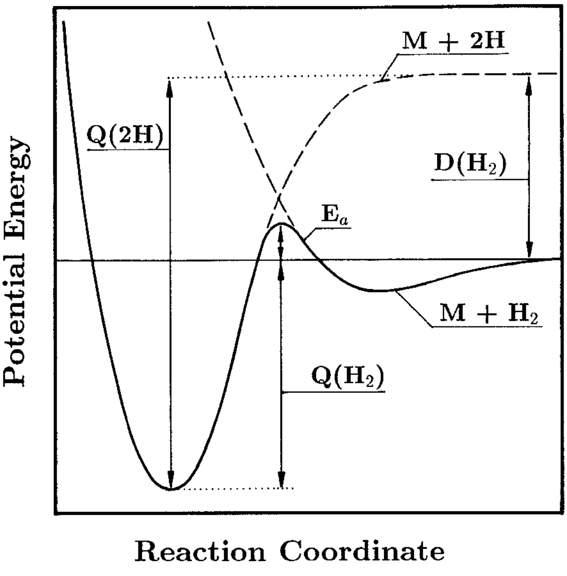

Figure 2. Schematic one-dimensional energy diagram for dissociative adsorption of hydrogen. The interaction potential of the molecule with the metal provides a shallow precursor state. Since during adsorption the dissociation of the H_2 molecule into two H atoms occurs, the overall potential energy diagram has to be appropriately scaled (mass scaling). All energies are counted per hydrogen molecule (H_2 or 2H). $Q(2H)$: binding energy of the two H-atoms; $Q(H_2)$: heat of adsorption for H_2; $D(H_2)$: dissociation energy for H_2; E_a: activation energy of adsorption for H_2.

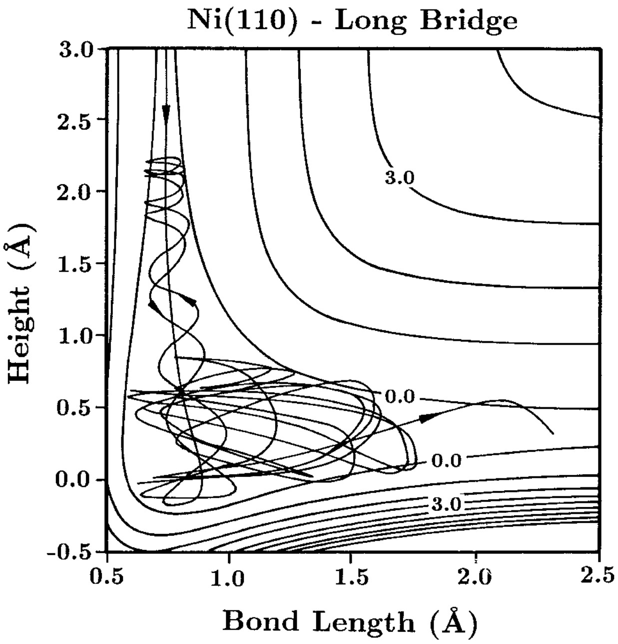

Figure 3. Representation of a classical trajectory in a two-dimensional potential energy diagram from Lee and De Pristo 1986. The calculations have been performed for hydrogen molecules impinging at a long bridge site on Ni(110). Obviously adsorption proceeds without an activation barrier between the gas phase and the adsorbed state, but multiple collisions are necessary before dissociation occurs. The potential energies are depicted in eV.

parallel to the surface and the rotational degrees of freedom are usually neglected. The surface itself is frequently treated as a two or more-atom cluster and the molecule is assumed to hit the surface at an on-top or bridge position (Harris 1988). Only very recently first attempts to study multidimensional effects (e.g. molecular orientation, quantum state of the molecules) have been made (Nielsen *et al.* 1990). However, general trends and to some extent also quantitative experimental results can readily be predicted with the currently available theoretical tools.

2.2. *The influence of surface parameters on the sticking coefficient*

2.2.1. *Electronic surface structure*

The dissociative adsorption process for H_2 on metal surfaces is primarily determined by the electronic density near the surface. If a hydrogen molecule approaches a metal it first experiences a weak attractive Van der Waals interaction. This attractive potential always exists and is the cause for a possible physisorbed (precursor) state. As the fully occupied $1\sigma_g$ orbital of the hydrogen molecule penetrates the outer tail of the s or p electron wave functions of the metal a repulsive potential due to the Pauli exclusion principle arises (Pauli repulsion). The closer the molecule approaches the surface the larger the resulting energy gets. This represents the repulsive part of the activation barrier for dissociative chemisorption of hydrogen. The repulsive energy increases until the energy of the $1\sigma_u$ orbital mixing with the s or p electrons of the surface becomes energetically more favourable than the $1\sigma_g$–metal configuration.

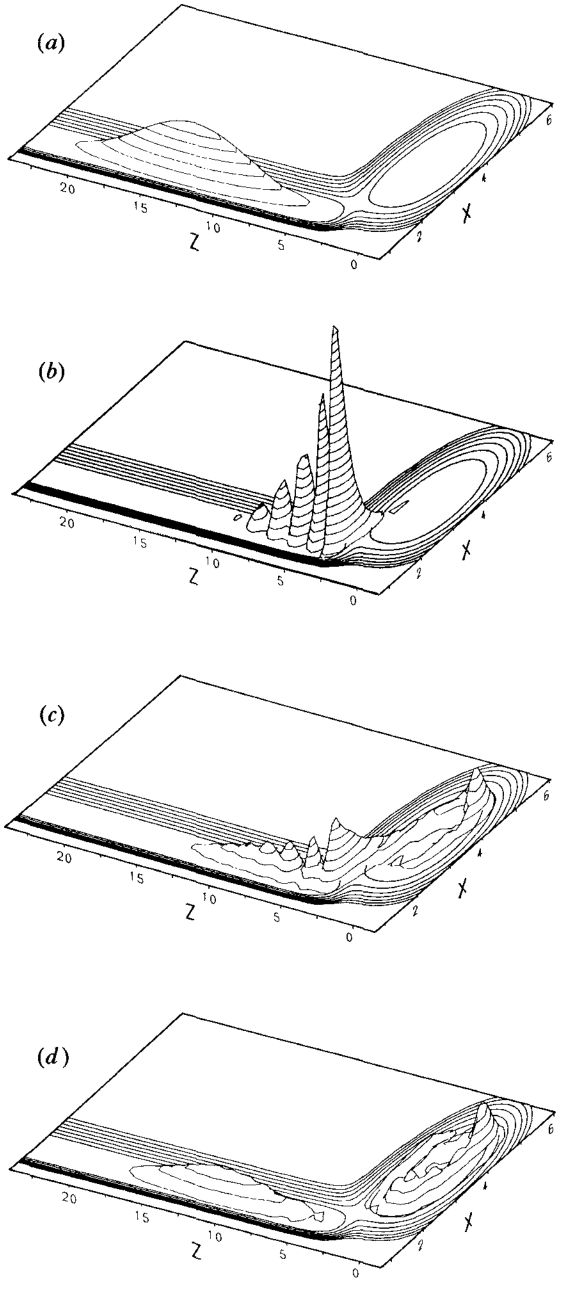

Figure 4. The sequence of pictures (*a*)–(*d*) shows the evolution in time of a wave packet approaching and transgressing an activation varrier for dissociative adsorption. Z is the distance between the H_2 molecule and the surface and X is the H–H separation, both in atomic units. (*a*) The molecule approaches the barrier through the entrance channel of adsorption. (*b*) About 72 fsec later the wave packet has reached the barrier. Partial reflection causes standing waves. (*c*) A further 41 fsec later part of the wave packet has transgressed the barrier. (*d*) About 30 fsec later the wave packet has split into an adsorbed and a reflected component. This beautiful 'movie' of an adsorption process has been computed by Kratzer and Brenig (1991).

The $1\sigma_u$ orbitals are antibonding with respect to the H–H bond but may be bonding in terms of an H–metal bond. In the adiabatic model one obtains an intersection of the H_2–metal potential curve and the H–metal potential (figure 2). In other words in transgressing the activation barrier the H–H bonds are weakened and the H–metal bonds are formed to result in two separately chemisorbed hydrogen atoms (Harris 1987, Hand and Holloway 1989a, b).

At this point one has to distinguish between adsorption on simple metals (e.g. Al) or noble metals (e.g. Cu) on the one hand and transition metals on the other hand (e.g. Ni). For simple and noble metals the adsorption proceeds exactly as described above; the result is a rather high activation barrier on the order of 1 eV. Qualitatively the height of the activation barrier will increase with increasing electron density of the substrate surface as for example from Na through Mg to Al. A similar trend should exist in the sequence Cu, Ag and Au. In fact no adsorption of *molecular* hydrogen has been obtained up to now on silver and gold.

A quite different scenario comes into play for transition metal surfaces. These metals are characterized by unfilled d bands. Since the d electrons and the s electrons share a common Fermi level it is possible to transfer an s electron from the s band into the unfilled d band without energy cost (Harris 1988). If we recall that the Pauli repulsion is mainly determined by the far reaching s electrons the transfer of s electrons into the more localized d electron shell will significantly decrease the repulsive part of the physisorption well and hence decrease the activation barrier for chemisorption. The sticking coefficient for H_2 on transition metal surfaces is by an order of magnitude larger than on simple or noble metal surfaces (Christmann 1988). Actually chemists have long known about the role of d band holes for the catalytic activity of transition metals (Bond 1972).

2.2.2. *Geometric surface structure*

The geometric and electronic structure of a surface are of course closely related, nevertheless, the influence of the geometric structure on the sticking coefficient is quite different on simple or noble metals on the one hand and on transition metals on the other. For the former surfaces the activation barrier for dissociation is usually very high (≈ 1 eV) due to the high s electron density on the surface. A change of this electron density through a change of the geometric packing density will not influence the activation barrier height dramatically. For the transition metal surfaces, however, the geometric effect is much more pronounced due to the possibility of s–d electron transitions. Whereas on the densely packed surfaces (e.g. f.c.c.-(111) planes) an activation barrier still exists in the range of several tenths of an electron volt, the repulsive barrier is reduced for the open transition metal surfaces (e.g. f.c.c.(110)) in such a way that unactivated adsorption becomes possible. For a qualitative explanation of the fact that rough transition metal surfaces often exhibit very low activation barriers, generally a similar reasoning is applied as the Smoluchovsky treatment of work function changes due to geometric variations (Smoluchovsky 1941).

Parallel to the reduction of the activation barrier often a deeper physisorption well is formed (see figure 2). Therefore nonactivated adsorption systems very often exhibit a pronounced precursor mediated adsorption kinetics.

2.2.3. *Surface defects and impurities*

The considerations in the preceding section can also be applied to the influence of surface defects. Again on noble and simple metal surfaces defects do not play such a dominant role as on transition metal surfaces. On the latter surfaces small amounts of defects can change the adsorption kinetics from an activated process to an unactivated process. In particular on densely packed transition metal surfaces adsorption may take place predominately on defect sites (Rendulic *et al.* 1987b, Rendulic 1988, Rendulic and Winkler 1989, Wandelt 1991). Examples for this behaviour will be given in section 4.

In the context of the local electron density influencing the activation barrier height it is easy to understand that foreign atoms on the surface will influence the sticking probability in different ways. Electropositive adatoms will give up negative charge to the metal surface giving rise to a local positive electrostatic potential. This change of the electrostatic potential is equivalent to a decrease in the local work function. The decrease results in a lower Pauli repulsion barrier and an increased electron transfer probability into the antibonding levels of the molecule and hence in a decrease of the activation barrier for dissociation (Bonzel 1984). Contrary, electronegative adatoms will increase the activation barrier for dissociative adsorption (Lundqvist 1983, Nørskov *et al.* 1984). While this picture of electronegative and electropositive adsorbates as inhibitors and promotors for most adsorption systems is certainly true, one has also to consider the specific adsorption site on which the adsorbate is located. Oxygen according to this picture should be an inhibitor. As will be shown in section 4 this is indeed true for surfaces that allow unactivated adsorption as for example the open (110) f.c.c.-surfaces or stepped surfaces. In contrast, on the flat Ni(111) surface which exhibits activated adsorption the oxygen can act as promotor of H_2 adsorption. In this case in the next vicinity of the electronegative adsorbate a zone of decreased electron density is created leading to a decrease of the activation barrier (Brown *et al.* 1991).

2.2.4. *Surface temperature*

To get trapped on the surface an impinging molecule has to get rid of its excess energy. This accommodation process will generally depend on surface temperature. As long as the adsorption well is deep enough, as in the case of dissociative chemisorption of hydrogen, the dissipation of energy poses no problem. As a consequence straight chemisorption of hydrogen (without a precursor) is generally not dependent on surface temperature (King 1978).

A totally different situation arises if the adsorption proceeds through an intermediate molecular precursor state. These precursors which are physisorbed (Van der Waals) states or lightly chemisorbed states exhibit rather shallow potential wells with a depth of perhaps a few kcal $(\mathrm{mol})^{-1}$. Here a distinct dependence of the sticking coefficient on surface temperature exists:

(1) The accommodation or dissipation of the excess kinetic energy depends on surface temperature (Goodman 1975).
(2) Once trapped in the precursor state the transition probabilities into the chemisorbed state or for desorption are temperature dependent (Kisliuk 1958).

First a discussion of the accommodation process: To release the excess energy of the molecule essentially two mechanisms may be effective. Phonon excitation is the most effective mechanism if the mass ratio between the adsorbate and the substrate atoms is not too small. Various models are in use to describe energy accommodation by phonon excitation (hard sphere, soft cube, etc.) (Goodman 1975, Grimmelmann *et al.* 1980). The effect of surface temperature can both increase as well as decrease the accommodation coefficient, depending on the specific circumstances.

For low mass adsorbates like hydrogen also electron–hole pair excitation might play a role in the accommodation process (Schönhammer and Gunnarsson 1981, Sols *et al.* 1984). When the impinging molecule with an initially unoccupied electronic state (the antibonding $1\sigma_u$ level of H_2) approaches the surface this level is downshifted below the Fermi level of the substrate and partially filled by electrons tunnelling out of the surface. Due to the lifetime of this process a temporarily electron–hole pair is generated. The accommodation probability due to e–h pair excitation should exhibit only a weak dependence on surface temperature. The reason is that two different effects cancel each other: Although the probability to release kinetic energy by the e–h pair production during the first round trip in the adsorption potential increases with temperature, energy gain in the following round trips by e–h pair annihilation decreases the probability to keep the molecule trapped (Schönhammer and Gunnarsson 1981).

For the molecule to get adsorbed on the surface only the velocity component normal to the surface (normal energy) has to be accommodated. The parallel component of the particle energy can be conserved upon impact, leading to a mobile adsorbate (hot precursor (D'Evelyn *et al.* 1987)). As a consequence of this physics a distinct variation of the sticking coefficient with the angle of incidence is encountered (see section 2.3.3.). The molecule once trapped in the precursor now moves freely across the surface. At each point on the surface the molecule possesses a certain probability to either chemisorb, desorb or migrate to another site. The relative heights of the activation barriers of each of these processes determine the temperature dependence of the overall sticking coefficient for dissociative chemisorption (Cassuto and King 1981).

So, while no *a priori* prediction of the surface temperature dependence of the sticking coefficient can be made, one can certainly state that whenever a surface temperature dependence is observed, precursor mediated adsorption is present.

2.2.5. *Surface coverage*

In the preceding sections we have strictly speaking dealt with the sticking coefficient in the zero coverage limit. This quantity is called the initial sticking coefficient. Although the integral initial sticking coefficient $\bar{S}_0$ characterizes the adsorption kinetics to some extent the coverage dependence of $\bar{S}$ yields additional information, in particular about adsorbate–adsorbate interactions. A compilation of integral initial sticking coefficients for H_2 on metal surfaces can be found in a review article by Christmann (1988). Only in a few instances has $\bar{S}_0$ been measured to be unity or close to unity, by far the majority of H_2–metal systems are characterized by initial sticking coefficients much smaller than one.

By increasing the amount of adsorbed particles N_{ad} on the surface the sticking coefficient normally decreases until at saturation coverage N_{sat} the sticking coefficient approaches zero. For direct dissociative adsorption the coverage dependence of the sticking coefficient can be written in the following form:

$$\bar{S}(N_{ad}) = (1 - N_{ad}/N_{sat})^2. \qquad (1)$$

This expression simply takes into account the available free space for dissociative (two particle) chemisorption. There are only few examples where the experimental data can be described by this functional dependence. When an impinging gas molecule is temporarily trapped in a precursor state (physisorbed state) then several attempts for dissociative adsorption can take place before the molecule desorbs from the surface. In the precursor state the molecule can migrate along the surface to find empty chemisorption sites where dissociative adsorption can occur. Kisliuk (1958) formulated the coverage dependence of the sticking probability for a precursor mediated adsorption:

$$\bar{S}(\vartheta)=\frac{\bar{S}_0(1-\vartheta)^2}{1-\vartheta(1-K)+\vartheta^2\bar{S}_0}, \tag{2}$$

where $\vartheta=N_{\mathrm{ad}}/N_{\mathrm{sat}}$, $\bar{S}_0=P_{\mathrm{a}}/(P_{\mathrm{a}}+P_{\mathrm{b}})$, $K=(P'_{\mathrm{b}}-P_{\mathrm{a}})/(P_{\mathrm{a}}+P_{\mathrm{b}})$, with P_{a} the dissociation probability on an empty chemisorption site, P_{b} the desorption probability from the precursor state over an empty chemisorption site, and P'_{b} the desorption probability from the precursor state over an occupied chemisorption site.

In figure 5 a set of $\bar{S}(N_{\mathrm{ad}})$ curves according to the Kisliuk model with different parameters K can be seen. Particularly the weak coverage dependence of $\bar{S}$ at low surface coverage, which is typical for precursor assisted adsorption, can be found rather frequently in the experiment.

In the Kisliuk model it is assumed that dissociation from a precursor state above an occupied chemisorption site is impossible. However, there exists experimental evidence that in specific situations the dissociation probability over occupied sites is even larger than over unoccupied sites (promotors for adsorption, see section 2.2.3.). A modification of the Kisliuk model can be used to describe the effect of promoting agents on the surface (Winkler and Rendulic 1982). In the context of this extended adsorption model sticking coefficients increasing with surface coverage can be modelled (autocatalytic process). Situations as such have been actually found for some adsorption systems (Winkler and Rendulic 1982, Winkler *et al.* 1988).

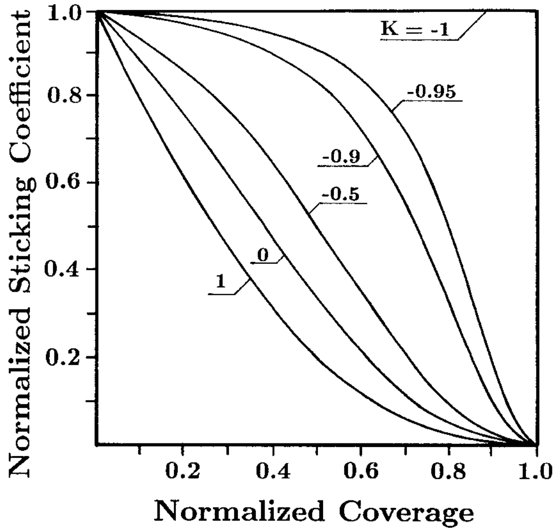

Figure 5. Coverage dependence of the sticking coefficient according to the model by Kisliuk 1958. The parameter K contains the desorption probability from occupied chemisorption sites according to the definition in the text (equation (2)). The smaller the desorption probability from occupied sites gets the more independent of coverage becomes the sticking probability.

Unfortunately, for many adsorbates the situation is much more complicated, so that $\bar{S}(N_{ad})$ cannot be described with one of the models presented. There are several scenarios which can be visualized but are difficult to formulate in a mathematical model:

(*a*) Steps and other defects on the surface may influence the sticking coefficient in a dramatic way at low coverages. At higher coverages the defects are blocked and adsorption is again dominated by sticking on the flat terraces (Wagner 1979).

(*b*) Adsorption may proceed into different adsorption sites even on a perfect surface. The coverage dependence of these distinct sites can be quite different (Somorjai 1981).

(*c*) Attractive and repulsive lateral interactions in the adsorbate can influence the sticking coefficient as function of coverage (Cassuto and King 1981).

(*d*) The adsorbate on the surface can be arranged in several coexisting phases (e.g. lattice gas and condensed phase) leading to distinct features in the adsorption kinetics (Payne and Kreuzer 1988).

(*e*) Reconstruction of the surface due to the adsorbate can expose new adsorption sites with totally different adsorption probabilities (Ladas *et al.* 1988).

2.3. *The influence of gas parameters on the sticking coefficient*

2.3.1. *Translational energy*

The kinetic energy of gas molecules impinging on a surface can influence the sticking probability in two different ways. For adsorption systems where no or only a small activation barrier for dissociative adsorption exists and the adsorption is *precursor mediated* the sticking coefficient is governed by the accommodation coefficient of the molecule in the precursor. The importance of the accommodation (dissipation) of the excess translational energy of the impinging molecule has already been discussed in section 2.2.4. For all accommodation processes (energy dissipation by phonon excitation or electron–hole pair excitation) theory predicts a decrease of the accommodation coefficient with increasing translational energy (Schönhammer and Gunnarsson 1981, Tully 1981). The decrease of the sticking coefficient with beam energy is indeed observed for many adsorption systems (Rettner *et al.* 1990). The effect is especially pronounced for very low translational energies ($E<0{\cdot}1\,\mathrm{eV}$) of the adsorbing molecules. Actually the occurrence of $\partial S/\partial E<0$ is a clear indicator of the presence of a precursor.

The opposite translational energy dependence is found when an activation barrier exists between the gas phase and the adsorbed phase. Then the probability to overcome the activation barrier increases with increasing translational energy. In the simplest case where a pure entrance channel barrier exists which in addition is independent of the position in the surface unit cell we encounter a one-dimensional activation barrier. Although this extreme assumption is usually not justified, the picture of a one-dimensional activation barrier is frequently used to deduce a mean activation barrier E_a from the experimental results (Van Willigen 1968). In a classical picture the translational energy dependence of the sticking coefficient will then exhibit a step function with $S=0$ for $E_{kin}<E_a$ and $S=1$ for $E_{kin}>E_a$, assuming an accommodation coefficient of unity. For adsorption of hydrogen of course quantum effects will allow tunnelling through the barrier even for $E_{kin}<E_a$ and for $E_{kin}>E_a$ the transition probability can be smaller than one. Then the $S(E_{kin})$ dependence is given by a typical

S-shape behaviour. Harris (1989) has proposed the following function to fit the translational energy dependence of the sticking coefficient:

$$S(E_{\mathrm{kin}})=\frac{1}{2}\left[1+\tanh\left(\frac{E_{\mathrm{kin}}-E_{\mathrm{a}}}{W}\right)\right], \tag{3}$$

with W as a rounding parameter which defines the width of the **S**-shaped curve.

In the one-dimensional picture for activated adsorption (without a precursor) only the normal component of the translational energy is used to transgress the activation barrier (normal energy scaling). However, if the molecule can be trapped temporarily in a physisorption well (or perhaps a transition state) then scrambling of the normal and parallel components of the translational energy can lead to a dependence of the sticking probability on total energy rather than normal energy (Auerbach *et al.* 1984, Gadzuk and Holloway 1985). In general of course the sticking coefficient as a function of translational energy has to be calculated using full classical trajectory treatments (Lee and De Pristo 1987) or quantum mechanical wave packet treatments (Hand and Holloway 1989a, b) on reasonably assumed potential energy surfaces.

2.3.2. *Vibrational energy*

In dissociative chemisorption immediately one question arises. What happens to the internal energy (vibration, rotation) of the molecule during dissociation? Can it perhaps be used to aid transgression of the activation barrier? Indeed theoreticians have long been predicting an influence of vibrational energy on the adsorption dynamics (Polanyi 1959). A conversion of vibrational energy into translational energy can come about in two different ways:

1. A softening of the potential to which the vibrating atoms of the adsorbing molecule (e.g. hydrogen) are subjected will lead to a decreased vibrational energy at constant vibrational quantum number. This energy released can be converted into translational energy which is used to transgress the activation barrier (Müller 1987, Halstead and Holloway 1990).
2. If the adsorption path in the PES is curved, a mixing of vibrational energy and translational energy can occur. Here the vibrational quantum number has to change. One can understand this mechanism even in a classical picture. For example a desorbing particle possessing translational energy will climb up the potential well in the curved section of the desorption path leading to a vibrational motion. The reverse process in adsorption, although more difficult to visualize, is of course equally possible (Halstead and Holloway 1990).

To experimentally check on the influence of the vibrational quantum state on the adsorption process molecular beams have to be used for which internal energy and translational energy can be adjusted independently (see section 3). The results show that for hydrogen the molecules in the first excited vibrational state have a vastly larger sticking coefficient than particles in the ground state. This difference can approach two orders of magnitude in the sticking coefficient.

A different approach to this problem can be gained through optical methods. In principle a molecular beam impinging on the surface can be conditioned by optical pumping (Farrow and Chandler 1988). Adsorbing, desorbing and scattered beams can be probed with respect to their rotational and vibrational population using REMPI (resonance enhanced multi photon ionization) (Zacharias 1990).

2.3.3. *Angle of incidence*

In the pioneering work of Van Willigen (1968) it was experimentally demonstrated for the first time that the angular distribution of desorbing molecules does not obey a pure cosine distribution. In addition, because of detailed balancing, the sticking coefficient can also be expected to change with the angle of incidence. This has been experimentally verified many times since (Palmer *et al.* 1970, Steinrück *et al.* 1985). In the picture of a one-dimensional activation barrier it is easy to understand that only the normal component of the translational energy is relevant for sticking, leading to the largest value of the sticking coefficient near the surface normal. This behaviour is called normal energy scaling (NES) and can be formulated through the expression:

$$S(E, \Theta) = S(E \cos^2 \Theta, 0^\circ). \tag{4}$$

The experiments show that for almost all hydrogen adsorption systems normal energy scaling is obeyed quantitatively or at least qualitatively. The implication of equation (4) is that for a given energy dependence of the sticking coefficient $S(E, 0^\circ)$ the angular variation of the sticking coefficient is uniquely determined. The steeper the dependence $S(E)$ the more forward focused will be the function $S(\Theta)$.

Traditionally the angular variation of the sticking coefficient $S(\Theta)$ has been represented by the approximation:

$$S(\Theta) \cos \Theta \propto \cos^n \Theta. \tag{5}$$

According to this definition and equation (4) a sticking coefficient of the form

$$S(\Theta) \propto \cos^{n-1} \Theta \tag{6}$$

will lead to an energy dependence of the sticking coefficient in the form (Anger *et al.* 1989):

$$S(E) \propto E^{(n-1)/2}. \tag{7}$$

The condition of normal energy scaling is generally also fulfilled for precursor mediated adsorption dynamics. The observed condition $\partial S/\partial E < 0$ leads to exponents $n < 1$ in the angular variation of the sticking coefficient. Since $n = 1$ means a sticking coefficient independent of the angle of incidence, values $n < 1$ exhibit sticking coefficients *increasing* with the angle Θ to the surface normal. Obviously identical physics is obtained by either decreasing the beam energy or by increasing the angle of incidence (see for example section 4).

2.3.4. *Isotope effect*

Any isotope effect caused by a specific adsorption process should be most pronounced for the hydrogen isotopes (H_2, D_2, T_2) where the highest mass ratios between all isotopes are encountered. Since for the individual adsorption processes the mass effect might be different, experiments using isotopes could give direct evidence for the specific process under work. A variety of physical processes during adsorption can yield an isotope effect:

(1) For direct activated adsorption without tunnelling the sticking coefficient only depends on the energy of the incoming molecule, therefore no isotope effect can be expected in this case. However, if tunnelling plays an essential role then the sticking probability should be higher for the lighter isotope.

(2) Vibrationally assisted adsorption also will exhibit a pronounced isotope effect. Under certain circumstances (see section 2.3.2) vibrational energy can be converted into translational energy, contributing to easier transgression of the activation barrier. In particular:

   (*a*) The energy of corresponding vibrational levels is higher for H_2 than for D_2. This will favour adsorption of H_2.

   (*b*) The population of equivalent vibrational levels is higher for D_2 than for H_2 at the same experimental conditions, which favours adsorption of D_2.

   (*c*) Finally the whole dynamics of vibrational energy transfer might differ for H_2 and D_2.

   The first two points mentioned above are counteracting processes which have been shown to partially compensate each other (Küchenhoff *et al.* 1991).

(3) Precursor mediated adsorption is influenced by the process of energy accommodation which will depend on the mass of the impinging particles. Phonon excitation will favour heavier masses; electron–hole pair excitation will favour the lighter mass at *identical translational energy* of the particles (Sols *et al.* 1984).

(4) Finally any process depending on surface migration of an adsorbate will favour the lighter isotope.

Actually, in most experimental investigations only very small isotope effects within the margin of error have been detected for the hydrogen isotopes. Only recently in the investigation of vibrationally assisted adsorption clear isotope effects for the individual vibrational states could be detected (Berger *et al.* 1991, Berger and Rendulic 1991).

3. Experimental determination of the sticking coefficient

The integral sticking coefficient is defined as the ratio of the adsorption rate R_{ads} to the impingement rate Z of an isotropic gas on a surface:

$$\bar{S}=\frac{R_{\mathrm{ads}}}{Z}. \tag{8}$$

Therefore the conventional way to determine the sticking coefficient is to measure both the amount of adsorbed particles and the number of impinging particles per unit surface area and unit time. For an isotropic gas the impingement rate per unit surface area is correlated with the gas pressure in the following way:

$$Z=\frac{\mathrm{d}N_{\mathrm{imp}}}{\mathrm{d}t}=\frac{p}{(2\pi mkT)^{1/2}}, \tag{9}$$

with p: gas pressure, m: mass of the gas particles, T: gas temperature and k: Boltzmann's constant.

According to equation (9) an absolute pressure measurement is necessary to obtain *absolute numbers of impinging particles*. The calibration of pressure gauges (ionization gauges) in the near ultra-high vacuum (UHV)-region is possible using the spinning rotor gauge (Fremerey 1985) with accuracies better than ±5%. Uncalibrated pressure gauges however can exhibit uncertainties of up to 100%.

To obtain the *number of adsorbed particles* in principle every coverage dependent signal like a work function change or the Auger electron yield etc. can be used. For adsorption of hydrogen, besides the fact that no Auger effect is possible, the most frequently used method is the thermal desorption spectroscopy (Redhead 1962). In this case the temperature of the hydrogen covered sample is increased, leading to desorption of the adsorbed gas particles. As a consequence the pressure temporarily rises in the vacuum chamber until all of the bound hydrogen is desorbed. The time integral of the pressure increase Δp is a measure of the amount of gas adsorbed per unit surface area:

$$N_{\mathrm{ad}}=\frac{KQ}{A}\int \Delta p\,\mathrm{d}t. \tag{10}$$

Conversion factor $K=2{\cdot}47\times10^{19}$ (molecules (mbar l)$^{-1}$) at 293 K, Q is the pumping speed in the vacuum system and A the surface area investigated.

There are basically two possibilities to determine absolute coverage values N_{ad}. The procedure can be performed straightforwardly if the effective pumping speed in the vacuum chamber is known, but unfortunately determination of this quantity is a rather difficult task. The second approach uses a calibration of the pressure integral in equation (10) by introducing an accurately known amount of gas into the vacuum chamber. We have developed a relatively simple but very accurate calibration method using synthetic flash desorption spectra (Winkler 1984, 1987). A glass vessel connected to the vacuum chamber via a valve can be backfilled with hydrogen gas and the pressure in the glass vessel can be measured absolutely using a spinning rotor gauge. This form of pressure measurement does not influence the gas phase in any way (e.g. through pumping or heating effects). From the volume of the glass vessel and the absolute pressure the number of enclosed hydrogen molecules can be determined. The valve is then opened to the vacuum chamber where the instreaming gas produces a temporary pressure burst. The integral $\int\Delta p\,\mathrm{d}t$ of this synthetic flash is directly correlated with the total amount of gas molecules introduced from the glass chamber. Simple comparison of the pressure integrals for the synthetic flash and the desorption spectra of interest then allows quantitative determination of the number of adsorbed particles. Since the everyday use of synthetic flash spectra is impracticable, secondary standards can be calibrated which allow a quick and easy absolute determination of the desorbing particles. It turns out that the hydrogen saturation coverage on a properly cleaned tungsten filament is highly reproducible. Once the saturation desorption spectrum for hydrogen from the tungsten filament is determined with the experimental method described above, this saturation spectrum can easily be used for comparison with the spectra of interest. Repeated calibration of the tungsten filament has demonstrated that an accuracy of ±5% for the saturation coverage can be obtained over many years (Winkler 1987).

However, there is one additional factor which may reduce the accuracy of the sticking coefficient measurements: the effective area of the sample surface where adsorption takes place might be ill defined. Careful preparation of the sample is necessary by cleaning only the front surface using argon sputtering where the rear surface and the rim of the sample remain contaminated. Nevertheless, the unknown effective surface area is most frequently the reason for an incorrectly measured sticking coefficient using thermal desorption techniques.

In addition to integral sticking coefficients $\bar{S}$ with isotropic gas supply differential sticking coefficients $S(T)$ or $S^{*}(E)$ for directional gas supply can be measured using collimated molecular beams. In this case the elegant method of King and Wells (1974) allows absolute determination of the sticking coefficient. When a molecular beam enters a vacuum chamber the pressure increase corresponds to the rate of inflowing gas molecules. If now the sample is brought into the cross-section of the beam a certain amount of particles adsorbing on the sample surface is removed from the gas phase resulting in a pressure drop. The percentage of the pressure drop is the numerical value of the sticking coefficient. The evolvement of the pressure change in time can be used to determine the sticking coefficient as a function of coverage. An important point in measurements according to King and Wells is the fact that no calibration in terms of pumping speed or particle numbers is needed.

The method of King and Wells is applicable only for adsorption systems with large sticking coefficients ($S > 0{\cdot}1$). For very small sticking coefficients a different method can be applied which also allows absolute determination of the sticking coefficient without the knowledge of the pumping speed. In this case the number of particles impinging on the surface from a collimated molecular beam is determined in arbitrary units of $\int \Delta p \, \mathrm{d}t$. A subsequent flash desorption experiment determines the adsorbed amount of particles in the same arbitrary units of $\int \Delta p \, \mathrm{d}t$. The ratio of the two pressure integrals directly yields the sticking coefficient; pumping speed and gauge sensitivity do not enter into the procedure. Obviously this method is especially suited for small sticking coefficients that do not produce a measurable effect according to King and Wells.

Molecular beams to determine differential sticking coefficients can be obtained from capillary arrays, Knudsen cells or free jet nozzle sources (Scoles 1988). From a Knudsen cell and a capillary array the effusing gas is Maxwellian and the energy distribution is characterized by the temperature of the cell, if only the gas pressure is low enough to stay in the molecular flow region. The mean energy of the particles of a Maxwellian flux then is

$$E = 2kT. \qquad (11)$$

Frequently Knudsen cells consist of a molybdenum tube with an effusion hole ($\approx 100\,\mu$m in diameter) laser machined radially into the tube wall. The tube can be heated resistively up to 2000 K and cooled with LN_2. The same arrangement can be used as source in a nozzle beam apparatus. In producing a supersonic nozzle beam the pressure in the nozzle is around 1 bar and several differentially pumped stages are necessary to reduce the pressure between the nozzle chamber ($\approx 10^{-4}$ Torr) and the UHV chamber ($\approx 10^{-10}$ Torr). Due to the continuum expansion of the gas isentropic cooling yields a quasi monoenergetic molecular beam. The mean translational energy of a monoenergetic beam is obtained through the conversion of the enthalpy contained in the high pressure gas into the expanding beam (Anderson 1974):

$$E = U + pV = \frac{3}{2}kT + kT = \frac{5}{2}kT, \qquad (12)$$

with U the internal energy and pV the mechanical work.

In this case it is assumed that rotational and vibrational relaxation is of no effect. Actually total or partial relaxation of the rotational energy (kT) can increase the translational energy to values between $5kT/2$ and $7kT/2$. Conversion of vibrational energy into translational energy can be neglected under normal experimental conditions in the case of hydrogen (Scoles 1988).

While the normal procedure to vary the energy for a monoenergetic nozzle beam is to vary the nozzle temperature (equation (12)) it is sometimes desirable to change the translational energy independently of nozzle temperature. This can be achieved with so-called seeded beams (Abuaf *et al.* 1967). Imagine a nozzle beam of a light gas originating from a nozzle of temperature T. If we inject a small amount of heavy gas into the light gas the heavy gas will experience an aerodynamic acceleration. The process can be turned around of course to slow down a light gas mixed into a heavy gas. Applications for seeded beams are the production of high energetic beams at relatively low nozzle temperatures. A further area of interest accessible through seeded beams is the investigation of vibrationally assisted sticking. Vibrational states (determined by the nozzle temperature T) and translational energy (determined by the mixing ratio of the gas in the seeded beam) can be varied independently to obtain state resolved sticking coefficients.

4. Sticking of H_2 on transition metal surfaces (nickel)

One of the most frequently investigated adsorption systems is undoubtedly hydrogen–nickel. It can be considered a model system for the adsorption of hydrogen on transition metal surfaces. Nevertheless, remarkable differences in the available data concerning the adsorption kinetics can be found in the literature (Christmann 1988). The strong dependence of the adsorption kinetics on surface parameters like structure, defects and impurities is responsible for this peculiarity.

The most impressive result concerning the influence of surface structure can be seen in figure 6. Here the initial sticking coefficient for H_2 on the three low index nickel surfaces as function of beam energy is presented (Rendulic *et al.* 1989, Rendulic and Winkler 1989). In particular at low kinetic energy there is a difference in the initial sticking coefficient of two orders of magnitude between Ni(110) and Ni(111).

The flat Ni(111) surface is characterized by a sticking coefficient increasing with increasing beam energy. At very low beam energy ($E_{\mathrm{kin}} < 0{\cdot}02\,\mathrm{eV}$) the sticking coefficient is actually zero. This result is characteristic for an activated adsorption

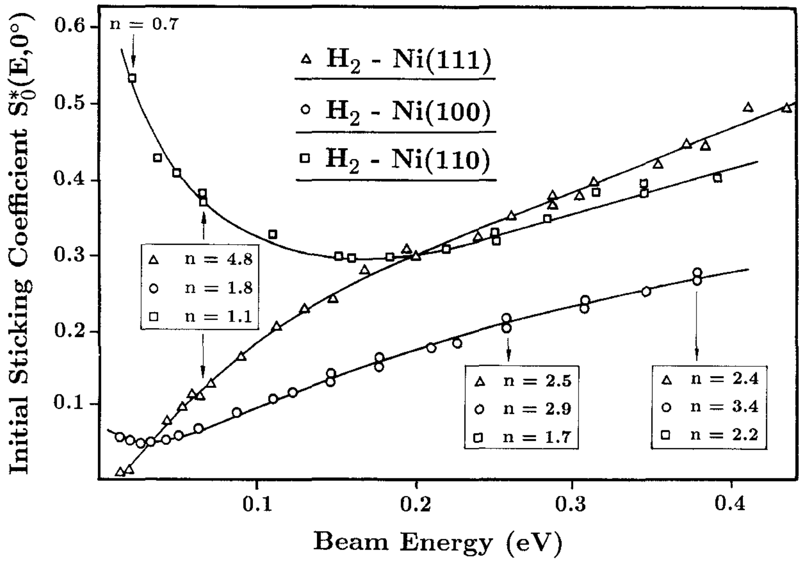

Figure 6. Initial sticking coefficients for monoenergetic hydrogen beams as function of beam energy on various nickel single crystal surfaces. The numbers n in the diagram indicate the exponent of the angular distribution according to equation (5). On the Ni(111) surface adsorption is activated ($\partial S/\partial E > 0$) whereas on the Ni(110) surface adsorption proceeds mainly through a non-activated precursor path ($\partial S/\partial E < 0$).

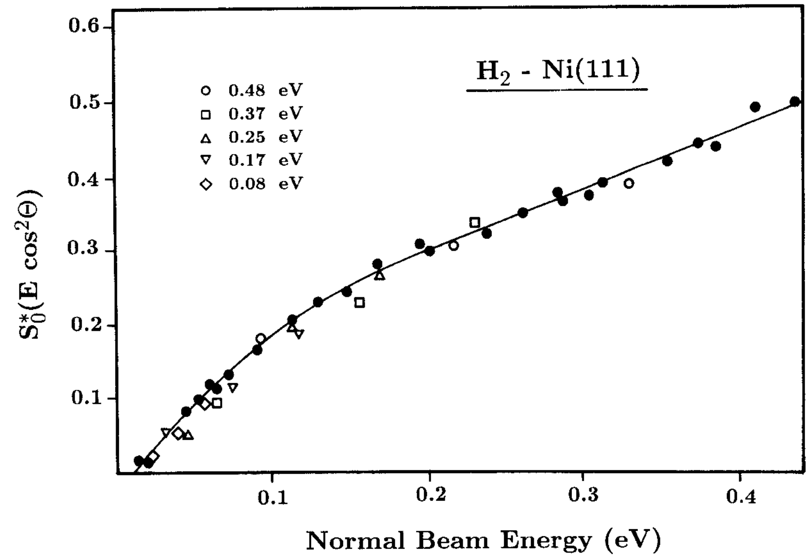

Figure 7. Test of normal energy scaling for H_2 on Ni(111). The full circles are the data points for the sticking coefficient of a monoenergetic beam at normal incidence as function of energy. The data for higher angles (open symbols) are plotted against normal energy ($E_n = E \cos^2 \Theta$) and coincide very well with the sticking coefficients for normal incidence.

process. On the flat, densely packed Ni(111) surface an activation barrier is formed due to the high electron density of the far reaching 4s electron shells. Although for transition metals the unfilled d band allows an s–d conversion which reduces the activation barrier (Harris 1988), a finite activation barrier remains on the Ni(111) surface. For the densely packed plane a more or less one-dimensional activation barrier can be expected which would yield a pronounced **S**-shaped energy dependence of the sticking coefficient (see equation (3)). Since this is obviously not the case one can conclude that a barrier height distribution across the surface unit cell must exist as suggested by Karikorpi *et al.* (1987) or Holloway (1987). The barrier height distribution ranges from 0·02 eV to 0·2 eV (Rendulic *et al.* 1989).

In figure 6 the angular distribution as characterized by the exponent *n* according to equation (5) is inserted for different beam energies. Interestingly, measurements of the angular variation of the sticking coefficient demonstrate that normal energy scaling (NES) is fulfilled for H_2–Ni(111) with rather good accuracy. In figure 7 the projection of the angle resolved sticking data into the curve $S_0^*(E, 0°)$ according to equation (4) is performed. As can be seen in this figure the plot of the sticking coefficient as function of normal energy ($E_n = E \cos^2 \Theta$) yields a single curve indicating the validity of normal energy scaling (NES) for this adsorption system.

For the Ni(110) surface, which is a loosely packed corrugated plane, the $S_0^*(E_{\text{kin}})$ dependence is quite different, particularly at low beam energies. Here the sticking coefficient increases with decreasing translational energy of the beam. This behaviour is characteristic of a precursor mediated adsorption process. At low beam energy accommodation into the physisorption well and subsequent indirect dissociative adsorption governs the overall adsorption process. On the strongly corrugated (110) surface the s–d conversion is most pronounced in the region of the protruding surface atoms. This shifts the Pauli repulsive barrier closer to the surface selvedge resulting in a decrease of the activation barrier and generation of a pronounced physisorption well. However, in figure 6 we see that still part of the surface allows direct activated adsorption at high beam energy: the sticking coefficient increases with beam energy. From the angular dependence, we see that not only for the activated regime ($n > 1$ and $\partial S/\partial E > 0$) but also for the non-activated precursor regime ($n < 1$ and $\partial S/\partial E < 0$) normal energy scaling is basically fulfilled.

The Ni(100) plane is a rather smooth surface where in fact the adsorption process is predominately activated. But from figure 6 we see that in contrast to the Ni(111) plane at low beam energy part of the impinging molecules can adsorb *via* a precursor state. Actually, in all experiments concerning the three nickel planes we find that the adsorption behaviour of the (100) plane exhibits a combination of features of both the (111) and the (110) surfaces.

The pronounced effect of the crystallographic orientation on the sticking coefficient directly leads to the suspicion that also surface defects may influence the adsorption process. Adsorption near surface defects has attracted considerable interest because of the possible role of defects as catalytically active sites. Indeed, on the (111) plane the sticking coefficient is changed dramatically by the introduction of surface defects (Rendulic *et al.* 1987). The defect density on the surface can be changed by applying different sputtering and annealing cycles. The integral initial sticking coefficient $\bar{S}_0$ on a softly sputtered but well annealed surface is 0·02, on an extensively sputtered but not adequately annealed surface the initial sticking coefficient is increased by more than a factor of three to 0·07 (Rendulic and Winkler 1989).

Defect sites on a surface can be produced in a more controlled fashion using stepped surfaces (Wagner 1979, Rendulic and Winkler 1989). Such a surface can be obtained by polishing a crystal tilted by several degrees with respect to a low index surface. If a (111) plane is cut by an angle of 6·5° one obtains a (997) surface or in a different notation (Lang *et al.* 1972) a $[9(111)\times(11\bar{1})]$ surface. This indicates that the surface consists of (111) terraces nine atom rows wide terminated by monoatomic steps of $(11\bar{1})$ orientation (figure 8). A similar vicinal plane is the (445) or $[8(111)\times(100)]$ plane. In

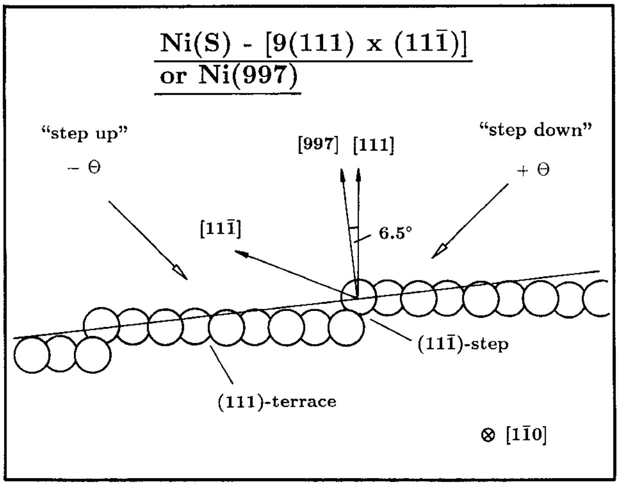

Figure 8. Atomic structure of a (997) plane of a f.c.c. crystal which can be considered a stepped (111) surface. The terraces are nine atom rows wide and separated by monoatomic steps of $(11\bar{1})$ orientation.

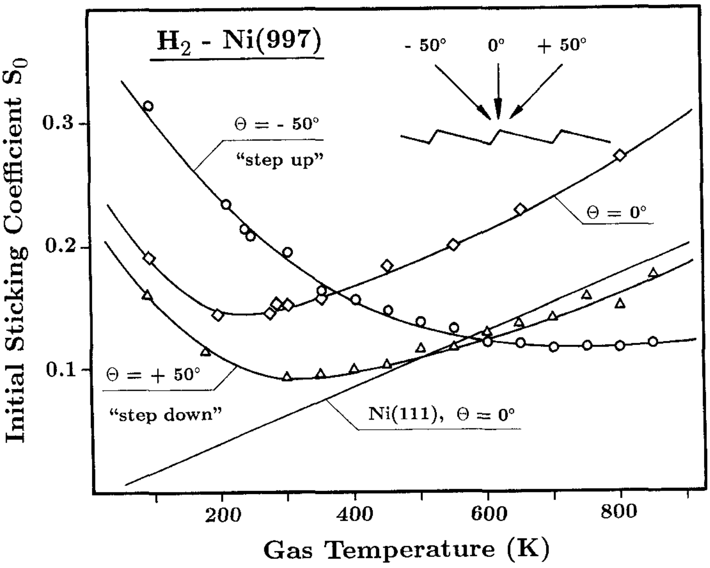

Figure 9. Initial sticking coefficient for a Maxwellian hydrogen beam on a Ni(997) surface as function of beam energy. Measurements are performed at three different angles of incidence as indicated in the insert. Depending on the angle of incidence either step sites or terrace sites are probed by the beam. Step sites ($\Theta = -50°$) yield mainly non-activated precursor adsorption whereas terrace sites ($\Theta = +50°$) exhibit mainly activated adsorption, similar to the undamaged Ni(111) plane.

both cases the defect density (concentration of atoms located at the step site) is about 10–15%. Surface steps and kinks within the steps are in addition to one-dimensional defects (adatoms, vacancies) the most important surface defects. The integral sticking coefficient for H_2 on a stepped (445) surface is 0·24, this means an increase by a factor of twelve compared with $\bar{S}_0 = 0{\cdot}02$ for the flat (111) surface (Winkler and Rendulic 1982). Defect sites on the more open planes like the Ni(110) surface obviously play a minor role since even on a flat surface the predominant process is the unactivated precursor mediated adsorption ($\bar{S}_0 = 0{\cdot}44$) (Steinrück *et al.* 1985a).

The pronounced influence of steps on a (997) plane for the sticking coefficient can also be seen in figure 9 (Karner *et al.* 1985). A Maxwellian beam is used which is characterized by the gas temperature. The initial sticking coefficient as function of beam energy is measured for three different angles of incidence. If the beam is pointed step-up ($\Theta = -50°$) mainly the step sites are probed by the beam. The sticking coefficient decreasing with increasing gas temperature is a clear indication of precursor assisted adsorption. The role of surface defects (steps) on a Ni(111) surface is to introduce sites for non-activated, precursor mediated adsorption on a surface showing otherwise only activated adsorption. When on the other hand the beam is pointed step down ($\Theta = +50°$) the steps are shaded and the beam hits mainly the flat terraces. On the terraces predominately activated adsorption is encountered resulting in a sticking coefficient increasing with beam energy. Still some non-activated sites remain in the path of the beam as seen in the low temperature precursor adsorption.

From an additional measurement of the angular variation of the sticking coefficient on a stepped surface (Karner *et al.* 1985) one can deduce that the influence of the defect sites is rather localized. On the terrace sites and on the step sites activated and non-activated adsorption is possible in parallel processes. Surface migration of undissociated hydrogen molecules from the precursor at defect sites to the terrace sites seems to be negligible. This is consistent with the result that no precursor for the flat Ni(111) plane has been found (Steinrück *et al.* 1985b).

In addition to defects impurities on the surface also play an important role in the adsorption process on transition metal surfaces. Sulphur, oxygen and carbon are the most frequently observed impurities which accumulate on the surface either by segregation from the bulk or by adsorption from the residual gas phase. These electronegative components usually lead to a decreased sticking coefficient for hydrogen (Rendulic and Winkler 1978). As outlined in section 2.2.3 the electronegative particles take negative charge from the metal surface which increases the local electrostatic potential and hence leads to an increased activation barrier for adsorption.

As already mentioned the step sites on a Ni(111) plane are catalytically active centres for the dissociation of hydrogen molecules. In figure 10 the action of a catalytic inhibitor is presented (Winkler and Rendulic 1982). Oxygen preadsorbed on a stepped surface preferentially quenches the active step sites, resulting in a rapid decrease of the sticking coefficient with oxygen coverage. A similar action of oxygen is seen on the Ni(110) surface (figure 11) where the oxygen progressively blocks the non-activated adsorption sites.

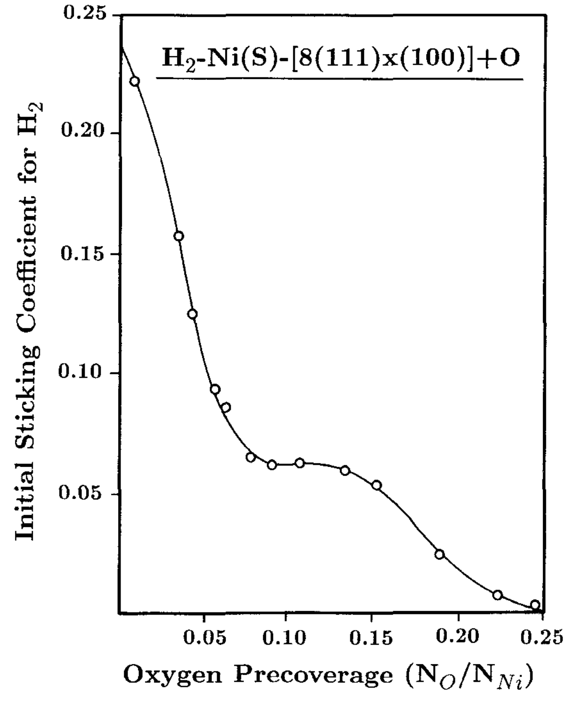

Figure 10. Initial sticking coefficient of hydrogen on a stepped nickel surface (Ni(445) or Ni(S)–[8(111)×(100)]) as function of oxygen precoverage. The rapid decrease of the sticking coefficient at low oxygen coverage is due to deactivation of the step sites by preferentially adsorbed oxygen. Only at higher oxygen coverage ($N_O/N_{Ni} > 0{\cdot}15$) additional blocking of the terrace sites leads to complete suppression of hydrogen adsorption.

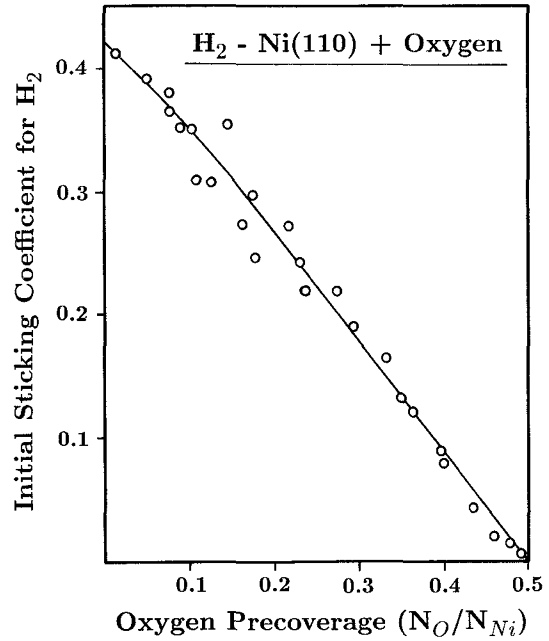

Figure 11. Initial sticking coefficient of H_2 on a Ni(110) surface as a function of oxygen precoverage. Since only non-activated adsorption sites are present on this surface simple blocking of these sites leads to the linear decrease of the sticking coefficient for H_2.

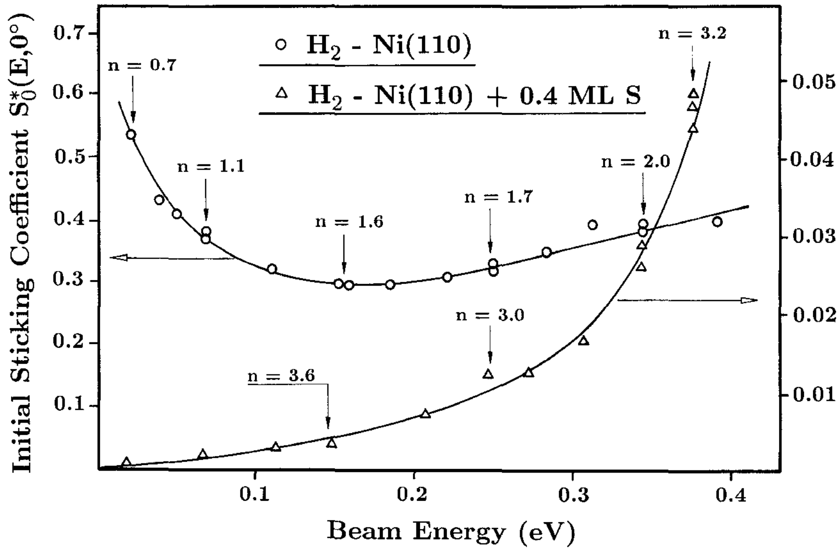

Figure 12. This diagram shows the physics involved in the action of a catalytic inhibitor. Hydrogen adsorption that can proceed through a non-activated, precursor mediated path on the clean Ni(110) surface ($\partial S/\partial E < 0$) becomes entirely activated ($\partial S/\partial E > 0$) after adsorption of 0·4 ML sulphur.

A more detailed picture of the action of inhibitors can be gained by the investigation of the adsorption dynamics on a nickel surface precovered with sulphur using molecular beam methods (Rendulic *et al.* 1989). In figure 12 the energy and angle dependence of the sticking for hydrogen on the Ni(110) surface is depicted. Upon sulphur precoverage the dynamics of adsorption is completely changed. The precursor mediated adsorption path originally present on the clean surface is completely suppressed. Adsorption on the sulphur covered surface is now purely activated. This can be deduced from the sticking coefficient increasing monotonically with beam energy. In addition the angular variation of the sticking coefficient is more forward peaked towards the surface normal on the sulphur covered surface (higher n values).

While the picture of the electronegative adsorbates as an inhibitor of hydrogen adsorption is quite plausible, one also has to take into account the role of different substrates. Oxygen preadsorbed on a flat Ni(111) surface exhibits both the properties of an inhibitor and a promotor. Apparently directly at the oxygen adsorption sites an inhibiting effect is encountered. However, in the next vicinity of the adsorption site the electronegative oxygen creates a zone of decreased electron density resulting in a reduction of the activation barrier (Brown *et al.* 1991). As a consequence low oxygen coverages enhance hydrogen adsorption (see figure 13) whereas at larger coverages the inhibiting effect dominates (Winkler and Rendulic 1982). A measurement of $S(T)$ and $S(\Theta)$ reveals the exact nature of the promoting action of preadsorbed oxygen on the chemisorption of hydrogen on the Ni(111) surface (figure 14). Preadsorption of oxygen

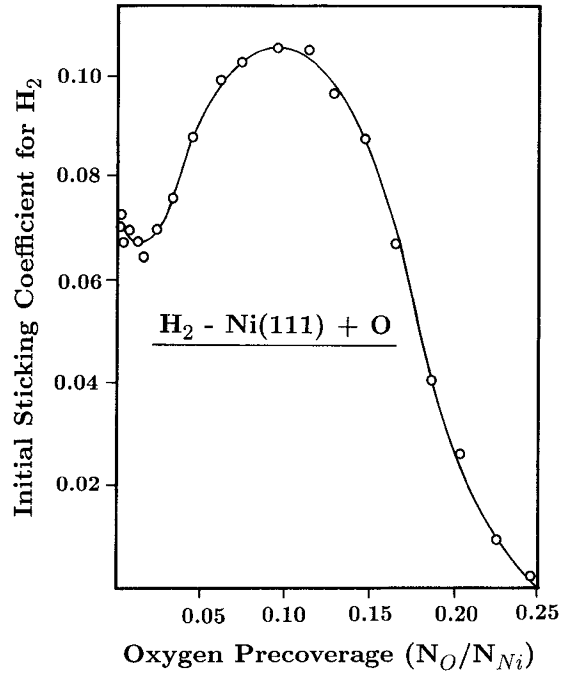

Figure 13. Initial sticking coefficient for hydrogen on Ni(111) as function of oxygen precoverage. For this particular adsorption system oxygen partially acts as promotor for adsorption: the sticking coefficient actually increases with oxygen coverage. Only at high oxygen coverage beyond 0·1 ML oxygen in addition acts as inhibitor and eventually completely suppresses the adsorption of hydrogen.

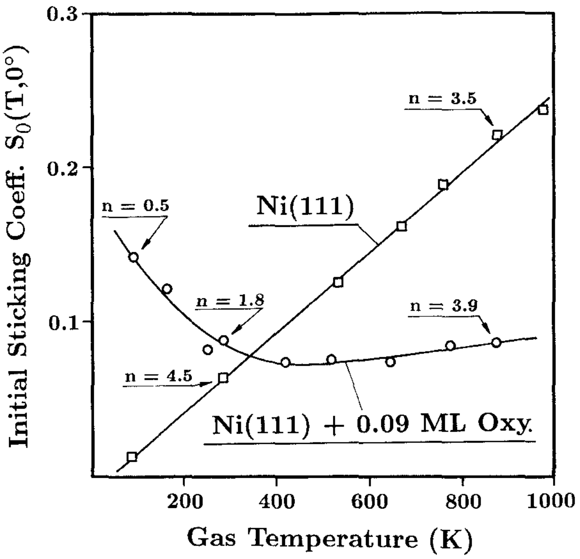

Figure 14. Initial sticking coefficient of a Maxwellian hydrogen beam on a clean and an oxygen precovered Ni(111) surface. Whereas on the flat (111) plane only activated adsorption is possible, on the partially oxygen covered surface a parallel, unactivated adsorption channel is opened. This can be recognized from the values $n < 1$ and the condition $\partial S/\partial E < 0$ for hydrogen adsorption on the oxygen precovered surface. In this model system the essence of a promotor of adsorption is manifested.

leads to a widening of the angular variation of the sticking coefficient (decrease of the exponent *n*) clearly indicating a *reduction of the activation barrier*. The values $\partial S/\partial T < 0$ for the oxygen covered surface indicates that adsorption sites for precursor mediated, nonactivated adsorption have been created in the vicinity of the adsorbed oxygen (Rendulic *et al.* 1987). One should note that the information contained in figure 14 describes essentially the opposite trend as contained in figure 12. From these two figures the different action of an inhibitor and a promotor of adsorption can best be recognized.

The properties of impurities on a surface as described above can be summed up in the following highlights: Coadsorbates (surface impurities) can act as promotors or inhibitors of hydrogen adsorption. Promoting action can be obtained only on surfaces which exhibit activated adsorption of hydrogen. On rough surfaces which allow non-activated adsorption to start with, the influence of promotors is of no importance. The mechanism of promotion is to reduce the activation barrier and to allow non-activated adsorption on a surface otherwise exhibiting a low sticking coefficient. An inhibitor, aside from simply blocking adsorption sites, can change the adsorption dynamics from a non-activated process to an activated process of low reaction rate. Whether an adsorbate acts as an inhibitor or promotor of hydrogen adsorption not only depends on the property of the impurity (electronegative or electropositive adsorbates) but also depends on the substrate surface under consideration. In some cases even a mixture of inhibiting and promoting effects may be observed.

Finally we want to discuss the possible influence of internal gas parameters like rotational and vibrational energy on the sticking coefficient for transition metal surfaces. Unfortunately, the experiments do not allow an unambiguous answer in the case of hydrogen adsorption on nickel. For a nozzle beam produced in a source at 1700 K the translational energy is about 0·3 eV and the sticking coefficient is in the range of 0·25–0·35 for all three nickel surfaces investigated. The number of molecules in the first excited vibrational state ($v=1$) is only about 3%. Even in the case of a differential sticking probability of unity the contribution of $v=1$ particles to the overall sticking coefficient would be below 10%. The only transition metal where an effect of $v=1$ hydrogen molecules to the sticking coefficient has been observed so far is iron (Berger *et al.* 1992). For H_2 molecules adsorbed on Fe(100) at a translational energy of 0·2 eV the state specific sticking coefficient for $v=0$ has been determined to be 0·03 whereas for $v=1$ molecules a state specific sticking probability of unity has been found.

5. Sticking of H_2 on noble metal surfaces (copper)

From the considerations outlined in section 2.2.1 we know that adsorption of hydrogen on noble metal surfaces (Cu, Ag, Au), if possible at all, proceeds with very low probability. Actually, from all noble metal surfaces only on copper surfaces has adsorption of H_2 been achieved up to now using high-energy molecular beams ($E_{\mathrm{kin}} > 0{\cdot}2$ eV). The adsorption probability of room temperature gas is below 10^{-5}. Apart from the early work of Balooch *et al.* (1974) only recently the H_2–copper system had attracted considerable interest. It has become a model system for vibrationally assisted adsorption (Anger *et al.* 1989, Hayden and Lamont 1989, Berger *et al.* 1990, Berger and Rendulic 1991, Hodgson *et al.* 1991, Rettner *et al.* 1991). The conversion of vibrational energy into translational energy and the utilization of this energy in activated chemisorption is of immense theoretical interest. In the long run also surface chemistry might profit from the investigation of vibrationally assisted adsorption, leading to improved process design. For this reason we are going to discuss this particular aspect of hydrogen adsorption on copper in some detail.

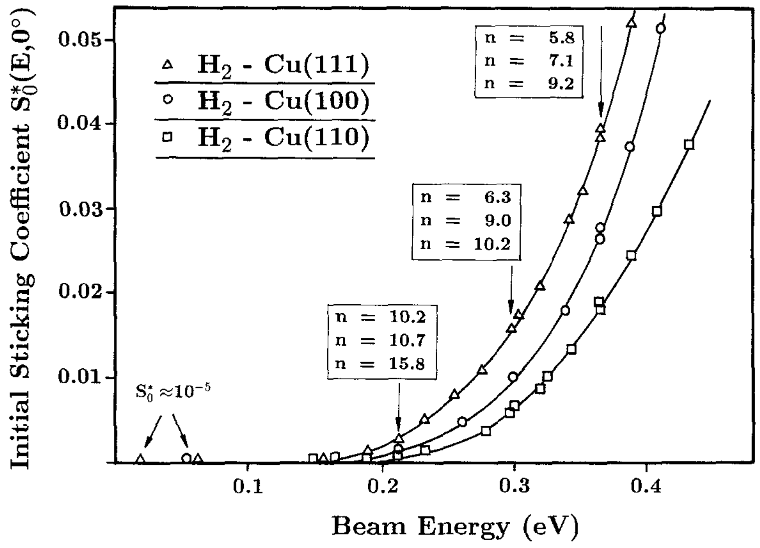

Figure 15. Initial sticking coefficient for a monoenergetic hydrogen beam as function of beam energy on various low index copper surfaces. The exponent n indicates the angular distribution of the sticking coefficient according to equation (5). The absence of adsorption at low translational energy and the high value of n demonstrate that adsorption is highly activated.

In figure 15 the translational energy dependence of the sticking coefficient for H_2 is shown for three copper surfaces (111), (110) and (100) (Anger *et al.* 1989). Compared with the similar representation for nickel (see figure 6) we observe the following features: for all three surfaces the sticking coefficient behaves rather similarly, no pronounced structural dependence can be seen. Below a translational energy of 0·2 eV the sticking coefficient is negligible, at higher beam energies S_0 increases monotonically to the experimentally highest attainable value of 0·05 at $E_{\mathrm{kin}} = 0{\cdot}4$ eV. Even at this high translational energy the sticking coefficient is by an order of magnitude smaller than on nickel. The angular distributions characterized by the exponents n according to equation (5) are also entered; very sharply forward peaked distributions are observed. The test of normal energy scaling (NES) for this adsorption system shows an interesting result (figure 16). Although a superficial inspection yields a rather good agreement for NES one can find a systematic deviation in particular for the scaled curves of high beam temperature. This is the first hint that in addition to the translational energy other terms might contribute to the adsorption process. Experiments using laser spectroscopy on *desorbing hydrogen molecules* (Kubiak *et al.* 1985) yielded abundant molecules in the vibrationally excited state $v = 1$. From detailed balancing considerations (Comsa 1977), molecules in the $v = 1$ state therefore should adsorb with higher sticking probability too.

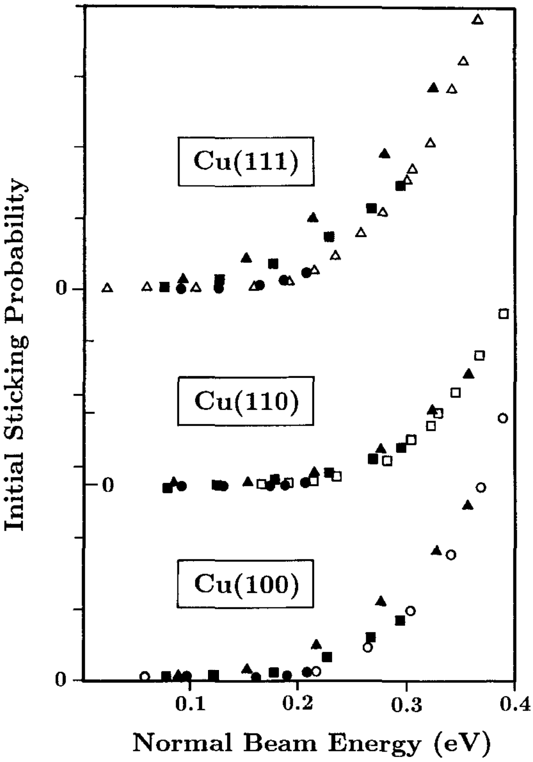

Figure 16. Test of normal energy scaling for H_2 on three copper single crystal surfaces. The open symbols are the data points for the sticking coefficient of a monoenergetic beam as function of energy at normal incidence. The filled symbols are data for higher angles of incidence plotted against $E_n = E\cos^2\Theta$. Distinct, systematic deviations from NES point towards the influence of vibrational contributions to adsorption.

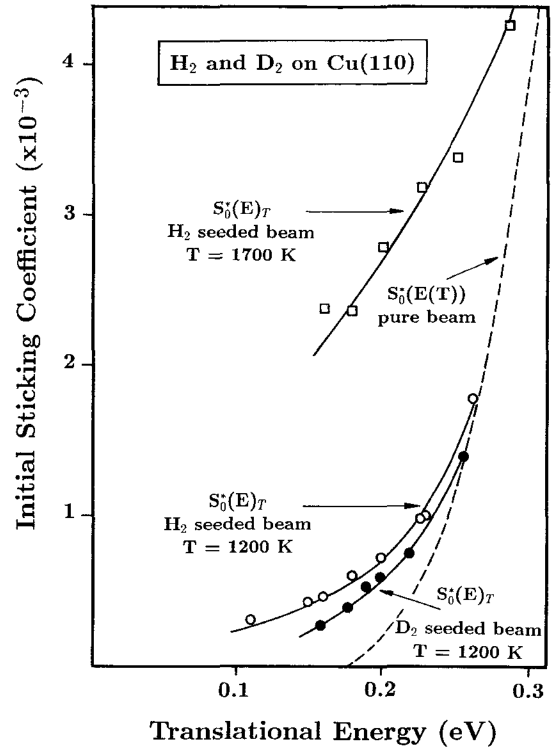

Figure 17. Due to vibrational contributions the sticking coefficient of hydrogen on copper becomes a function of both the translational energy and the internal energy (nozzle temperature). Only a set of curves $S(E)_T$ describes the adsorption system in a proper fashion. A plot of $S(E(T))$ as usually obtained in beam experiments (dashed line) does not characterize the physics completely.

The use of seeded beams described in section 3 allows partial decoupling of the translational energy and the vibrational energy. In figure 17 the influence of vibration to the sticking probability of H_2 on Cu(110) can be seen very clearly (Berger and Rendulic 1991, Rendulic 1992). The curve $S_0(E(T))$ is obtained using a conventional nozzle beam. In this case not only the translational energy increases with nozzle temperature but also the number of hydrogen molecules in the $v = 1$ state. If we use a seeded beam (H_2–Ne mixture) we can vary the translational energy at constant nozzle temperature, i.e. constant internal energy or constant number of molecules in $v = 1$. We recognize in figure 17 that the vibrationally hot beam originating from high nozzle temperature at 1700 K exhibits a higher sticking coefficient than the vibrationally colder beam at 1200 K. A very similar result has already previously been found for the adsorption system H_2–Cu(111) (Berger *et al.* 1990). The sticking coefficient is clearly a function of both translational energy and internal (vibrational) energy. Under these conditions an adsorption system has to be characterized by a set of sticking curves $S_0^*(E)_{T=\mathrm{const}}$ as indicated in figure 17. The conventional measurement $S_0^*(E(T))$ does not fully characterize the adsorption dynamics.

An equivalent representation is a plot of sticking coefficients as a function of temperature at constant translational energy (Berger and Rendulic 1991). Although experimentally more difficult to obtain, these curves yield information about the

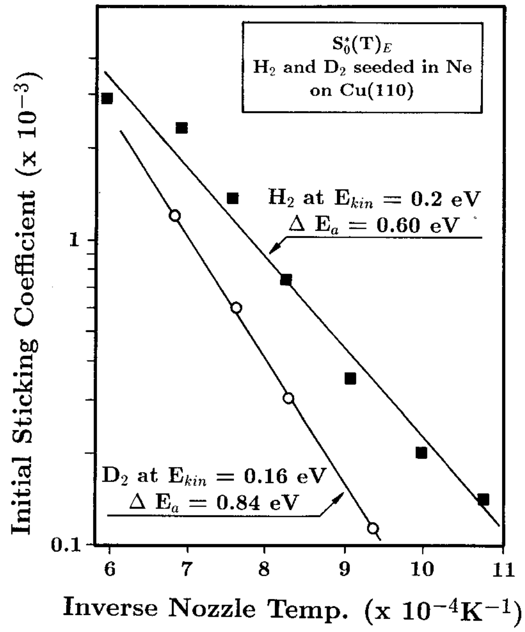

Figure 18. A plot of the temperature dependence of the sticking coefficient for H_2 and D_2 at constant translational energies. The variation of the sticking coefficient in this experiment is due solely to the change of the occupation numbers in the excited vibrational levels. The slope of the lines yields the activation energy to populate these levels. For hydrogen the experimentally obtained value $\Delta E_{\rm a}=0{\cdot}60$ eV is close to $\Delta E_{\rm a}(v_0 \rightarrow v_1)=0{\cdot}51$ eV, demonstrating that mainly molecules in the first excited vibrational level contribute to sticking. For deuterium the experimentally obtained $E_{\rm a}=0{\cdot}84$ eV is close to $\Delta E_{\rm a}(v_0 \rightarrow v_2)=0{\cdot}73$ eV, which shows that mainly deuterium molecules in the second excited vibrational level contribute to adsorption at the given translational energy and temperature.

particular vibrational states involved in adsorption. If one plots the logarithm of the temperature dependent part of the sticking coefficient *versus* $1/T$ one directly obtains from the slope the activation energy necessary to excite the molecules into the higher vibrational levels. The activation energy obtained from figure 18 is in the range of 0·6 eV for the H_2 molecular beam indicating that predominately molecules in the first excited state ($\Delta E_{\rm a}=0{\cdot}51$ eV for the difference between $v=0$ and $v=1$) contribute to the temperature variation of the sticking coefficient. Population of the state $v=2$ ($\Delta E_{\rm a}=1{\cdot}0$ eV) is apparently too small to contribute significantly to adsorption in this temperature and energy range. Also the contribution of rotational excitations seems to be of minor importance. This is in agreement with the results by Kubiak *et al.* (1985) who found that the rotational temperature of desorbing particles deviates only slightly from the surface temperature.

Based on the data in figure 18 one can deduce *state specific sticking probabilities* $S(E)_v$ for $v=0$ and $v=1$ molecules by simply relating the sticking coefficient as a function of temperature to the number of particles in the specific state (Berger *et al.* 1991). The result for H_2–Cu(110) is presented in figure 19. A dramatic difference between $S_0(E)_{v=1}$ and $S_0(E)_{v=0}$ can be observed. At a specific translational energy the sticking coefficient is by more than two orders of magnitude higher for $v=1$ than for $v=0$. From another point of view we can formulate that the effective adsorption barrier

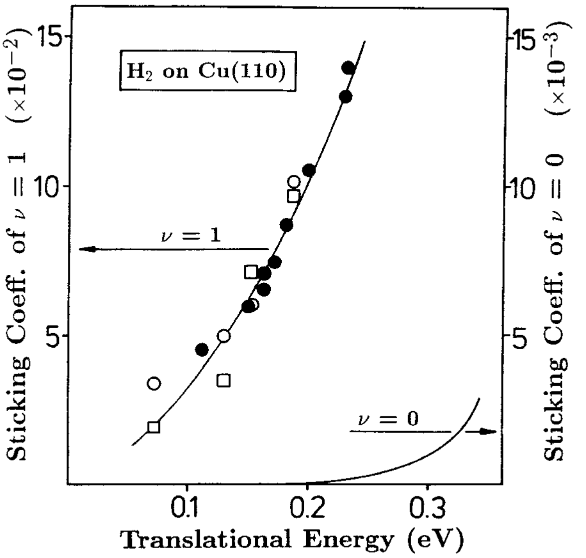

Figure 19. State resolved sticking coefficients for H_2–Cu(110). There is a vast difference in the sticking coefficients for H_2 in the ground state and the first excited vibrational state. Please note the difference of a factor 10 used in the scales for $v=1$ and $v=0$. Solid circles are directly measured points, open symbols are obtained for two different temperatures through normal energy scaling.

for $v=1$ particles is reduced by about 0·3 eV. That means that roughly 60% of the vibrational energy is converted into translational energy during the adsorption process.

Adsorption of deuterium should show a considerable isotope effect when compared with the dynamics of H_2–Cu. In particular in the representation $S(E)_T$ where the occupation of the individual vibrational levels stays fixed the difference in the sticking coefficient between the two isotopes will show up. In figure 18 the sticking coefficient for deuterium at a nozzle temperature of 1200 K is entered too. Sticking is reduced by up to 30–50% when compared to the equivalent hydrogen data. A similar experiment as shown for H_2 in figure 17 when performed for deuterium indicates that at a translational energy of 0·16 eV mainly deuterium in the vibrational state $v=2$ contributes to sticking ($\Delta E_a = 0{\cdot}72\,\mathrm{eV}$). An increase of the translational energy will eventually also lead to adsorption in the lower states $v=1$ and $v=0$ (Berger and Rendulic 1991). A measurement of $S(E(T))$ in contrast will not show such a pronounced isotope effect because the variation of the temperature not only increases the translational energy but also the occupation numbers in the individual vibrational states leading to partial compensation of the isotope effect. Küchenhoff *et al.* (1991) have performed quantum mechanical calculations using appropriate potential energy surfaces to determine sticking coefficients for H_2 and D_2 on copper. They obtained surprisingly good agreement between theory and experiment for the translational, vibrational and angular dependence of the sticking coefficient.

6. Sticking of H_2 on simple metal surfaces (aluminium)

The adsorption probability of molecular hydrogen on simple metal surfaces is exceedingly small under room temperature conditions. Most adsorption experiments therefore have been performed with atomic hydrogen. From the theoretical point of view it is immediately clear that due to the high electron density at the Fermi level the Pauli exclusion principle shifts the repulsive barrier for impinging molecules far away from the surface (Johansson 1981). The result is a very high activation barrier for dissociative adsorption. Only recently the use of high-energy molecular beams has allowed *molecular* adsorption of hydrogen on aluminium surfaces (Berger and Rendulic 1991). In figure 20 the initial sticking coefficient for hydrogen on Al(110) is shown as a function of translational energy. Up to 0·3 eV (corresponding to a nozzle temperature of 1400 K) no adsorption can be detected experimentally. Only above 0·3 eV the sticking coefficient starts to increase steeply. However, the highest experimentally attainable value for the sticking coefficient of H_2 is still only 4×10^{-4}. The high translational energy onset of adsorption and the very low sticking coefficient at the beam energies indicated points to an activation barrier for dissociative chemisorption in excess of 1 eV (Harris 1988).

It is clear that experiments for such low sticking coefficients are rather difficult to perform. Special care has to be taken to consider the coadsorption of atomic hydrogen which generally is assumed to exhibit a sticking coefficient of unity. In the hot nozzle of the molecular beam apparatus the degree of dissociation is determined by the nozzle temperature and the gas pressure in the nozzle. For the experimental conditions in use (maximum temperature $T = 1850$ K, $p = 0·5$ bar) one can calculate (Landolt–Börnstein 1968) the degree of dissociation to be 4×10^{-4}; this will lead to an adsorption rate in the same order of magnitude as the sticking coefficient for molecular hydrogen. The

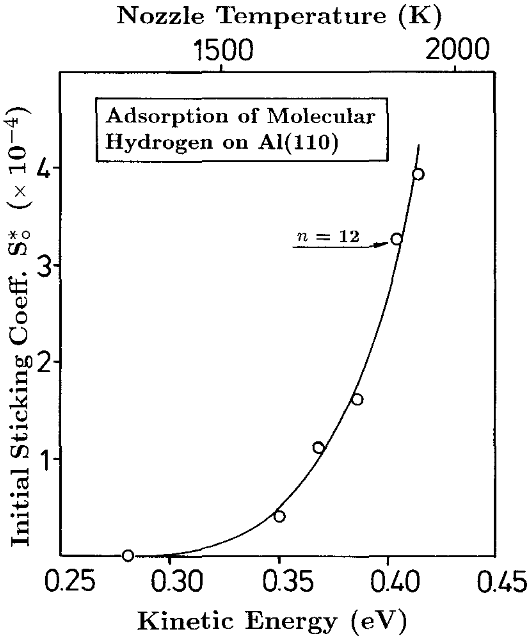

Figure 20. Initial sticking coefficient of a monoenergetic hydrogen beam on Al(110). The data points have been obtained by subtracting the atomic contribution to the apparent sticking coefficient (see figure 21). Note the small sticking coefficient, the high-energy onset of sticking and the sharply forward focused angular distribution characterized by the exponent n according to equation (5). This demonstrates that adsorption of H_2 on Al(110) is highly activated.

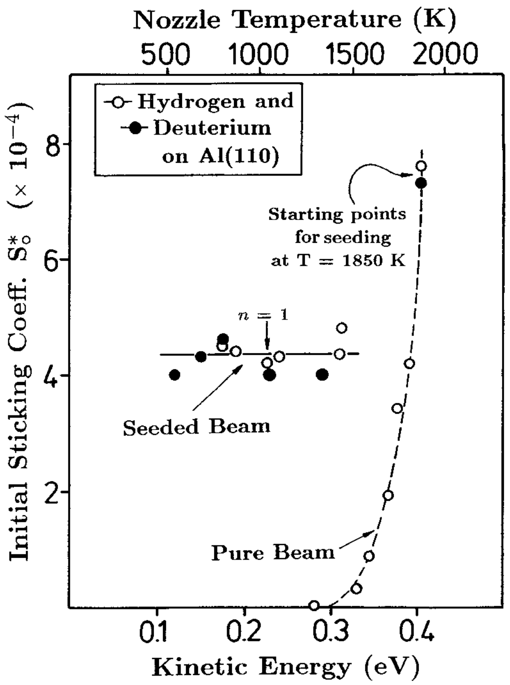

Figure 21. The apparent sticking coefficient of H_2 and D_2 on Al(110). Only part of the adsorbed hydrogen stems from H_2 (D_2) molecules, the rest originates from atomic hydrogen (deuterium). A seeded beam experiment is used to separate both contributions. For the cold-seeded beam at high nozzle temperature and low translational energy only the atomic fraction in the beam is able to adsorb. The cosine distribution of the angular variation of the apparent sticking coefficient for the seeded beam ($n = 1$) supports this result.

sticking coefficient presented in figure 20 was actually obtained by subtracting the contribution of atomic hydrogen from the raw sticking data. The contribution of atomic hydrogen can be determined by the use of a seeded beam probing the energy below 0·3 eV at nozzle temperatures above 1500 K. The apparent sticking coefficient will be *constant*, independent of energy and angle of incidence (figure 21): this is the contribution of atomic hydrogen to sticking. An actual experiment determining the temperature dependence of this constant contribution agrees very well with the trend expected from the law of mass action for thermal dissociation of hydrogen (Berger and Rendulic 1991).

A measurement of vibrational contributions to the sticking coefficient is very difficult in the presence of atomic hydrogen. However, the temperature and angle dependence of a vibrational contribution should be quite different from the contribution of atomic hydrogen. No such vibrational contribution can be detected within the margin of error for the system H_2–Al(110). If at all present, the vibrational contribution in the system H_2–aluminium would be very small.

The adsorption of hydrogen on aluminium shows another very interesting aspect that needs to be discussed. It is the formation of an aluminium hydride on the surface. Already electron energy loss spectroscopy (EELS) investigations have suggested the existence of aluminium hydrides on the hydrogen covered surface, in addition to straight chemisorbed dissociated hydrogen (Paul 1988). Thermal desorption of hydrogen from aluminium surfaces indeed shows H_2 molecules as well as AlH_x

compounds (Hara *et al.* 1991, Winkler *et al.* 1991b). These measurements have to be performed with a mass spectrometer *in line* with the desorption flux. Only under these circumstances the AlH_x compounds can be registered, otherwise the AlH_x decomposes upon deposition on the walls of the vacuum vessel; the *pressure signal* registered by the mass spectrometer *will not* contain hydrides.

One of the most interesting features arises from the phase equilibrium of lattice gas hydrogen with the hydride covered islands on the aluminium surface (Winkler *et al.* 1991b). Because of this phase equilibrium the H_2 desorption exhibits a zero reaction order: the rate of desorption is independent of the hydrogen surface coverage. In addition, an increase of the heating rate leads to a disturbance in the phase equilibrium and AlH_x compounds start to desorb from the edges of the hydride islands.

Finally one should point out a remarkable feature of the hydrogen adsorption on aluminium. As mentioned earlier the barrier for dissociative chemisorption determined in the molecular beam experiment is certainly larger than 1 eV. On the other hand the evaluation of the thermal desorption spectra yields a desorption energy of only 0·8 eV (Winkler *et al.* 1991a). This indicates that hydrogen on the aluminium surface is bound in a metastable state. The adsorbed hydrogen is in a state of higher energy than the free, gas phase, hydrogen.

7. Concluding remarks

The adsorption of hydrogen on metal surfaces is an experimentally intensively researched subject. In addition, the physics involved in the process of adsorption can be described rather well by theoretical models. All available data give a rather complete picture for most hydrogen–metal adsorption systems. Not only the adsorption dynamics on the undisturbed clean surface can be explained, but also the role of surface defects and surface contaminants in the catalytic activity for hydrogenation and dehydrogenation can be understood within the existing adsorption models. Molecular beam techniques have greatly contributed to the unravelling of many details of the adsorption process. After discovering the paramount influence of the quantum state of the molecule on the adsorption dynamics, the experimental methods are well on the way to investigate further intricate details as for example the influence of the molecular orientation on the adsorption process.

Acknowledgments

This work has been supported by the Austrian Fonds zur Förderung der wissenschaftlichen Forschung. Special thanks go to the many friends and co-workers who over the years have contributed to the material presented in the paper. Furthermore we are indebted to W. Brenig and P. Kratzer for letting us have the beautiful series of pictures in figure 4.

References

ABUAF, N., ANDERSON, J. B., ANDRES, R. P., FENN, J. B., and MILLER, D. R., 1967, *Proceedings Fifth International Symposium on Rarified Gas Dynamics*, edited by C. L. Brudin (New York: Academic).

ANDERSON, J. B., 1974, *Molecular Beams and Low Density Gasdynamics*, edited by P. P. Wegener (New York: Marcel Dekker).

ANGER, G., WINKLER, A., and RENDULIC, K. D., 1989, *Surf. Sci.*, **220**, 1.

AUERBACH, D. J., PFNÜR, H. E., RETTNER, C. T., SCHLAEGEL, J. E., LEE, J., and MADIX, R. J., 1984, *J. chem. Phys.*, **81**, 2525.

BALOOCH, M., CARDILLO, M. J., MILLER, D. R., and STICKNEY, R. E., 1974, *Surf. Sci.*, **46**, 358.

Berger, H. F., Grösslinger, E., and Rendulic, K. D., 1992, *Surf. Sci.*, **261**, 313.

Berger, H. F., Leisch, M., Winkler, A., and Rendulic, K. D., 1990, *Chem. Phys. Lett.*, **175**, 425.

Berger, H. F., and Rendulic, K. D., 1991, *Surf. Sci.*, **253**, 325.

Bond, G. C., 1972, *Principles of Catalysis* (London: Chemical Soc.).

Bonzel, H. P., 1984, *J. vac. Sci. Technol.* A, **2**, 866.

Brown, J. K., Luntz, A. C., and Schultz, P. A., 1991, *J. chem. Phys.*, **95**, 3767.

Cassuto, A., and King, D. A., 1981, *Surf. Sci.*, **102**, 388.

Christmann, K., 1988, *Surf. Sci. Rep.*, **9**, 1.

Comsa, G., 1977, *Proceedings Seventh International Vacuum Congress and Third International Conference on Solid Surfaces*, edited by R. Dobrozemsky *et al.* (Vienna), p. 1317.

D'Evelyn, M. P., Steinrück, H. P., and Madix, R. J., 1987, *Surf. Sci.*, **180**, 47.

Farrow, R. L., and Chandler, D. W., 1988, *J. chem. Phys.*, **89**, 1994.

Fremerey, J. K., 1985, *J. vac. Sci. Technol.* A, **3**, 1715.

Gadzuk, J. W., and Holloway, S., 1985, *Chem. Phys. Lett.*, **114**, 314.

Goodman, F. O., 1975, *Prog. Surf. Sci.*, **5**, 261.

Grimmelmann, E. K., Tully, J. C., and Cardillo, M. J., 1980, *J. chem. Phys.*, **72**, 1039.

Halstead, D., and Holloway, S., 1990, *J. chem. Phys.*, **93**, 2859.

Hand, M. R., and Holloway, S., 1989a, *J. chem. Phys.*, **91**, 7209; 1989b, *Surf. Sci.*, **211/212**, 940.

Hara, M., Domen, K., Onishi, T., Nozoye, H., Nishihara, C., Kaise, Y., and Shindo, H., 1991, *Surf. Sci.*, **242**, 459.

Harris, J., 1987, *J. vac. Sci. Technol.* A, **5**, 698; 1988, *Appl. Phys.* A, **47**, 63; 1989, *Surf. Sci.*, **221**, 335.

Harris, J., Rahman, T., and Yang, K., 1988, *Surf. Sci.*, **198**, L312.

Hayden, B. E., and Lamont, C. A., 1989, *Chem. Phys. Lett.*, **160**, 331.

Hodgson, A., Moryl, J., and Zhao, H., 1991, *Chem. Phys. Lett.*, **182**, 152.

Holloway, S., 1987, *J. vac. Sci. Technol.* A, **5**, 476.

Johansson, P. K., 1981, *Surf. Sci.*, **104**, 510.

Karikorpi, M., Holloway, S., Henriksen, N., and Nørskov, J. N., 1987, *Surf. Sci.*, **179**, L41.

Karner, H., Luger, M., Steinrück, H. P., Winkler, A., and Rendulic, K. D., 1985, *Surf. Sci.*, **163**, L641.

King, D. A., 1978, *CRC Critical Rev. Solid State Mater. Sci.*, **7**, 167.

King, D. A., and Wells, M. A., 1974, *Proc. R. Soc.* A, **339**, 245.

Kisliuk, P., 1958, *J. Phys. Chem. Solids*, **5**, 78.

Kratzer, P., and Brenig, W., 1991, private communication.

Kubiak, G. D., Sitz, G. O., and Zare, R. N., 1985, *J. chem. Phys.*, **83**, 2538.

Küchenhoff, S., Brenig, W., and Chiba, Y., 1991, *Surf. Sci.*, **245**, 389.

Ladas, S., Imbihil, R., and Ertl, G., 1988, *Surf. Sci.*, **198**, 42.

Landolt–Börnstein, 1968, Vol. 2/part 5, edited by K. Schäfer (Berlin: Springer), p. 360.

Lang, B., Joyner, R. W., and Somorjai, G. A., 1972, *Surf. Sci.*, **20**, 440.

Lee, C. Y., and De Pristo, A. E., 1986, *J. chem. Phys.*, **84**, 485; 1987, *J. vac. Sci. Technol.* A, **5**, 485.

Lennard-Jones, J. E., 1932, *Trans. Faraday Soc.*, **28**, 333.

Lundqvist, B. I., 1983, *Vacuum*, **33**, 639.

Müller, J. E., 1987, *Phys. Rev. Lett.*, **59**, 2943.

Nielsen, U., Halstead, D., Holloway, S., and Nørskov, J. K., 1990, *J. chem. Phys.*, **93**, 2879.

Nørskov, J. K., Holloway, S., and Lang, N. D., 1984, *Surf. Sci.*, **137**, 65.

Palmer, R. L., Smith, Jr, J. N., Saltsburg, H., and O'Keefe, D. R., 1970, *J. chem. Phys.*, **53**, 1666.

Paul, J., 1988, *Phys. Rev.* B, **37**, 6164.

Payne, S. H., and Kreuzer, H. J., 1988, *Surf. Sci.*, **205**, 153.

Polanyi, J. C., 1959, *J. chem. Phys.*, **31**, 1338.

Redhead, P. A., 1962, *Vacuum*, **12**, 203.

Rendulic, K. D., 1988, *Appl. Phys.* A, **47**, 55; 1992, *Surf. Sci.* (in press).

Rendulic, K. D., Anger, G., and Winkler, A., 1989, *Surf. Sci.*, **208**, 404.

Rendulic, K. D., Winkler, A., and Karner, H., 1987a, *J. vac. Sci. Technol.* A, **5**, 488.

Rendulic, K. D., and Winkler, A., 1978, *Surf. Sci.*, **74**, 318; 1989, *Int. J. mod. Phys.* B, **3**, 941.

Rendulic, K. D., Winkler, A., and Steinrück, H. P., 1987b, *Surf. Sci.*, **185**, 469.

Rettner, C. T., Auerbach, D. J., and Michelsen, H. A., 1992, *Surf. Sci.* (in press).

Rettner, C. T., Mullins, C. B., Bethune, D. S., Auerbach, D. J., Schweizer, E. K., and Weinberg, W. H., 1990, *J. vac. Sci. Technol.* A, **8**, 2699.

Schönhammer, K., and Gunnarsson, O., 1981, *Phys. Rev.* B, **24,** 7084.

Scoles, G., 1988, *Atomic and Molecular Beam Methods*, Vol. 1 (Oxford University Press).

Smoluchowsky, R., 1941, *Phys. Rev.*, **60,** 661.

Sols, F., Garcia, N., and Flores, F., 1984, *Surf. Sci.*, **146,** L577.

Somorjai, G. A., 1981, *Chemistry in Two Dimensions* (Ithaca: Cornell University Press).

Steinrück, H. P., Luger, M., Winkler, A., and Rendulic, K. D., 1985a, *Phys. Rev.* B, **32,** 5032.

Steinrück, H. P., Rendulic, K. D., and Winkler, A., 1985b, *Surf. Sci.*, **154,** 99.

Tully, J. C., 1980, *J. chem. Phys.*, **73,** 1975; 1981, *Surf. Sci.*, **111,** 461.

Van Willigen, W., 1968, *Phys. Lett.* A, **28,** 80.

Wagner, H., 1979, Physical and chemical properties of stepped surfaces. In *Springer Tracts of Modern Physics*, Vol. 85 (Berlin, Heidelberg, New York: Springer), p. 151.

Wandelt, K., 1991, *Surf. Sci.*, **251,** 387.

Winkler, A., 1984, *J. vac. Sci. Technol.* A, **2,** 1393; 1987, *Ibid.* A, **5,** 2430.

Winkler, A., Guo, X., Siddiqui, H. R., Hagans, P. L., and Yates, Jr, J. T., 1988, *Surf. Sci.*, **201,** 419.

Winkler, A., Požgainer, G., and Rendulic, K. D., 1991a, *Surf. Sci.*, **251/252,** 886.

Winkler, A., and Rendulic, K. D., 1982, *Surf. Sci.*, **118,** 19.

Winkler, A., Resch, Ch., and Rendulic, K. D., 1991b, *J. chem. Phys.*, **95,** 7682.

Zacharias, H., 1990, *Int. J. mod. Phys.* B, **4,** 45.